

Two-photon excitation and stimulated emission depletion by a single wavelength

Teodora Scheul, Ciro D'Amico, Irène Wang,* and Jean-Claude Vial

Univ. Grenoble 1 / CNRS, LIPhy UMR 5588, Grenoble, F-38041, France

*irene.wang@ujf-grenoble.fr

Abstract: Super-resolved optical microscopy using stimulated emission depletion (STED) is now a mature method for imaging fluorescent samples at scales beyond the diffraction limit. Nevertheless the practical implementation of STED microscopy is complex and costly, especially since it requires laser beams with different wavelengths for excitation and depletion. In this paper, we propose using a single wavelength to induce both processes. We studied stimulated emission depletion of 4-dicyanomethylene-2-methyl-6-p-dimethylaminostyryl-4H-pyran (DCM) dye with a laser delivering a single wavelength in the near infrared. Fluorescence was excited by two photon absorption with a femtosecond pulse, then depleted by one photon stimulated emission with a stretched pulse. Time-resolved fluorescence decay measurements were performed to determine the depletion efficiency and to prove that fluorescence quenching is not affected by side effects. Numerical simulations show that this method can be applied to super-resolved microscopy.

©2011 Optical Society of America

OCIS codes: (190.0190) Nonlinear optics; (260.2510) Fluorescence; (300.6500) Spectroscopy, time-resolved; (350.5730) Resolution; (000.2170) Equipment and techniques.

References and links

1. R. Heintzmann, T. M. Jovin, and C. Cremer, "Saturated patterned excitation microscopy--a concept for optical resolution improvement," *J. Opt. Soc. Am. A* **19**(8), 1599–1609 (2002).
2. S. W. Hell and J. Wichmann, "Breaking the diffraction resolution limit by stimulated emission: stimulated-emission-depletion fluorescence microscopy," *Opt. Lett.* **19**(11), 780–782 (1994).
3. S. W. Hell and M. Kroug, "Ground-state-depletion fluorescence microscopy: A concept for breaking the diffraction resolution limit," *Appl. Phys. B* **60**(5), 495–497 (1995).
4. M. G. Gustafsson, "Nonlinear structured-illumination microscopy: wide-field fluorescence imaging with theoretically unlimited resolution," *Proc. Natl. Acad. Sci. U.S.A.* **102**(37), 13081–13086 (2005).
5. M. J. Rust, M. Bates, and X. Zhuang, "Sub-diffraction-limit imaging by stochastic optical reconstruction microscopy (STORM)," *Nat. Methods* **3**(10), 793–796 (2006).
6. E. Betzig, G. H. Patterson, R. Sougrat, O. W. Lindwasser, S. Olenych, J. S. Bonifacino, M. W. Davidson, J. Lippincott-Schwartz, and H. F. Hess, "Imaging intracellular fluorescent proteins at nanometer resolution," *Science* **313**(5793), 1642–1645 (2006).
7. S. T. Hess, T. P. K. Girirajan, and M. D. Mason, "Ultra-high resolution imaging by fluorescence photoactivation localization microscopy," *Biophys. J.* **91**(11), 4258–4272 (2006).
8. B. Hein, K. I. Willig, C. A. Wurm, V. Westphal, S. Jakobs, and S. W. Hell, "Stimulated emission depletion nanoscopy of living cells using SNAP-tag fusion proteins," *Biophys. J.* **98**(1), 158–163 (2010).
9. U. V. Nägerl, K. I. Willig, B. Hein, S. W. Hell, and T. Bonhoeffer, "Live-cell imaging of dendritic spines by STED microscopy," *Proc. Natl. Acad. Sci. U.S.A.* **105**(48), 18982–18987 (2008).
10. K. I. Willig, B. Harke, R. Medda, and S. W. Hell, "STED microscopy with continuous wave beams," *Nat. Methods* **4**(11), 915–918 (2007).
11. V. Westphal, C. M. Blanca, M. Dyba, L. Kastrup, and S. W. Hell, "Laser-diode-stimulated emission depletion microscopy," *Appl. Phys. Lett.* **82**(18), 3125–3127 (2003).
12. D. Wildanger, E. Rittweger, L. Kastrup, and S. W. Hell, "STED microscopy with a supercontinuum laser source," *Opt. Express* **16**(13), 9614–9621 (2008).
13. E. Auksorius, B. R. Boruah, C. Dunsby, P. M. P. Lanigan, G. Kennedy, M. A. A. Neil, and P. M. W. French, "Stimulated emission depletion microscopy with a supercontinuum source and fluorescence lifetime imaging," *Opt. Lett.* **33**(2), 113–115 (2008).
14. W. Denk, J. H. Strickler, and W. W. Webb, "Two-photon laser scanning fluorescence microscopy," *Science* **248**(4951), 73–76 (1990).

15. G. Moneron and S. W. Hell, "Two-photon excitation STED microscopy," *Opt. Express* **17**(17), 14567–14573 (2009).
16. J. B. Ding, K. T. Takasaki, and B. L. Sabatini, "Supraresolution imaging in brain slices using stimulated-emission depletion two-photon laser scanning microscopy," *Neuron* **63**(4), 429–437 (2009).
17. Q. Li, S. S. Wu, and K. C. Chou, "Subdiffraction-limit two-photon fluorescence microscopy for GFP-tagged cell imaging," *Biophys. J.* **97**(12), 3224–3228 (2009).
18. S. C. Baer, "Single wavelength stimulated emission depletion microscopy," U.S. Patent 7,816,654 B2 (Oct. 19, 2010).
19. M. Lesiecki, F. Asmar, J. M. Drake, and D. M. Camaioni, "Photoproperties of DCM," *J. Lumin.* **31–32**, 546–548 (1984).
20. J. Kušba, V. Bogdanov, I. Gryczynski, and J. R. Lakowicz, "Theory of light quenching: effects of fluorescence polarization, intensity, and anisotropy decays," *Biophys. J.* **67**(5), 2024–2040 (1994).
21. R. J. Marsh, D. A. Armoogum, and A. J. Bain, "Stimulated emission depletion of two-photon excited states," *Chem. Phys. Lett.* **366**(3–4), 398–405 (2002).
22. S. W. Hell, "Increasing the resolution of far-field fluorescence light microscopy by point-spread-function engineering," *Top. Fluoresc. Spectrosc.* **5**, 361–426 (2002).
23. T. A. Klar, S. Jakobs, M. Dyba, A. Egner, and S. W. Hell, "Fluorescence microscopy with diffraction resolution barrier broken by stimulated emission," *Proc. Natl. Acad. Sci. U.S.A.* **97**(15), 8206–8210 (2000).
24. C. Xu and W. W. Webb, "Measurement of two-photon excitation cross sections of molecular fluorophores with data from 690 to 1050 nm," *J. Opt. Soc. Am. B* **13**(3), 481–491 (1996).
25. J. M. Drake, M. L. Lesiecki, and D. M. Camaioni, "Photophysics and cis-trans isomerization of DCM," *Chem. Phys. Lett.* **113**(6), 530–534 (1985).
26. I. Gryczynski, V. Bogdanov, and J. R. Lakowicz, "Light quenching of tetraphenylbutadiene fluorescence observed during two-photon excitation," *J. Fluoresc.* **3**(2), 85–92 (1993).
27. I. Gryczynski, J. Kušba, V. Bogdanov, and J. R. Lakowicz, "Quenching of fluorescence by light: A new method to control the excited-state lifetimes and orientations of fluorophores," *J. Fluoresc.* **4**(1), 103–109 (1994).
28. E. Rittweger, B. R. Rankin, V. Westphal, and S. W. Hell, "Fluorescence depletion mechanisms in super-resolving STED microscopy," *Chem. Phys. Lett.* **442**(4–6), 483–487 (2007).
29. P. R. Hammond, "Laser dye DCM, its spectral properties, synthesis and comparison with other dyes in the red," *Opt. Commun.* **29**(3), 331–333 (1979).
30. A. J. Bain, R. J. Marsh, D. A. Armoogum, O. Mongin, L. Porrè, and M. Blanchard-Desce, "Time-resolved stimulated emission depletion in two-photon excited states," *Biochem. Soc. Trans.* **31**(5), 1047–1051 (2003).
31. M. Dyba, T. A. Klar, S. Jakobs, and S. W. Hell, "Ultrafast dynamics microscopy," *Appl. Phys. Lett.* **77**(4), 597–599 (2000).
32. T. A. Klar and S. W. Hell, "Subdiffraction resolution in far-field fluorescence microscopy," *Opt. Lett.* **24**(14), 954–956 (1999).
33. X. Guo and A. Xia, "Ultrafast excited states relaxation dynamics in solution investigated by stimulated emission from a styryl dye," *J. Lumin.* **122–123**, 532–535 (2007).
34. K. D. Piatkevich, J. Hulit, O. M. Subach, B. Wu, A. Abdulla, J. E. Segall, and V. V. Verkhusha, "Monomeric red fluorescent proteins with a large Stokes shift," *Proc. Natl. Acad. Sci. U.S.A.* **107**(12), 5369–5374 (2010).

1. Introduction

Fluorescence microscopy is a central tool for life science investigations, allowing non-invasive *in vivo* observations. However, it has been known since Abbe that the lateral size (full-width at half maximum) of the spot focused by a lens is limited to $\lambda/(2NA)$ where λ is the wavelength of light and NA is the numerical aperture of the lens. Using visible light and knowing that the best objective lenses have a numerical aperture of $NA \sim 1.4$, this limit is about 200 nm in practice. This means that conventional optical microscopy cannot distinguish features smaller than 200 nm. In the last years, several methods, so-called super resolution microscopy methods, have emerged in order to break this limit [1–7], among which the concept of stimulated emission depletion (STED) microscopy is one of oldest and most promising. The principle of STED was first described by Hell and Wichmann in 1994 [2]. It uses two laser beams to control and confine fluorescence emission in a spot that can be much smaller than the diffraction limit. The fluorophores are excited with a focused laser pulse, then a second pulse with a doughnut shape is sent to deplete the population of the excited state by stimulated emission. Therefore fluorescence can only be emitted in the very center of the excited volume, where the depletion beam has zero intensity. This effectively reduces the size of the Point Spread Function (PSF) and increases spatial resolution. This technique can combine fast acquisition speed and high spatial resolution, providing, for example, live cell imaging with 50 nm resolution [8] and allowing 3D volume reconstruction [9]. However, STED microscopy generally requires a relatively complex and expensive setup, therefore simplifications are welcomed. So far, in all STED microscopes, excitation and depletion are

performed by two different wavelengths that are sent simultaneously into the microscope. These beams can be delivered by two different laser sources [10,11] or by a supercontinuum [12,13]. Since the most efficient versions of STED use pulsed lasers, when several sources are used, they must be temporally synchronized with a precision in the picosecond range. This is not the case when a supercontinuum is used since the different wavelengths are inherently synchronized. Another problem when using different wavelengths arises from the presence of chromatic aberration in most optical systems, which makes it difficult to focus and perfectly overlap all the beams in the microscope focal plane. These difficulties impede the wider use of STED microscopy.

Here we present a new concept that aims at simplifying the STED setup by using a single wavelength for both excitation and depletion. In our scheme, a femtosecond (fs) laser pulse populates the excited state of the molecules by a two-photon process, while the stimulated depletion of the excited state, by means of a one-photon process, is accomplished by a temporally stretched laser pulse. The fs and the stretched pulse come from the same source, a Ti:Sa oscillator, and are at the same wavelength. Therefore, this technique will be named SW-STED, for single wavelength stimulated emission depletion. Our approach combines STED and two-photon excitation (TPE) microscopy and aims at bringing the higher resolution afforded by STED to any TPE microscope without having to add another laser source.

Two-photon excitation (TPE) microscopy [14] is now a well-established microscopy technique with specific advantages. Due to the non-linear relationship between the light intensity and excitation efficiency, fluorescence is confined to the focal spot which leads to a reduction of photo-toxicity and photo-bleaching outside the focal plane. Compared to confocal configuration, TPE microscopy does not need pinholes to perform 3D imaging, since its reduced out-of-focus fluorescence results in direct axial sectioning. This leads to more efficient light collection in scattering media. Another advantage of TPE microscopy for biological applications comes from using wavelengths in the NIR region, allowing deeper penetration in scattering tissues.

The combination of TPE and STED techniques has already been reported [15–17]. However, these studies still use two laser sources to produce different wavelengths. As mentioned in [15], the merging of TPE with STED microscopy limits the choice of suitable light sources for applications, due to the high peak-power required for both excitation and depletion. For the moment the best choice is a mode-locked fs laser for excitation and an Optical Parameter Oscillator (OPO) for the STED beam. This combination of light sources is not only costly but also difficult to operate. As it has been pointed out in a recent patent [18], by using a single wavelength for both two-photon excitation and stimulated emission depletion, SW-STED would provide a significant simplification to the technique. It would solve the problems related to laser pulse synchronization, thermo-mechanical drifts of independent sources and achromatism of microscope objectives and wave-plates, since the two laser beams come from the same laser and have the same wavelength. Moreover, as only one wavelength has to be filtered out prior to detection, fluorescence signal collection is also simplified.

This article aims at testing the validity of SW-STED concept by measurements in solution and numerical simulations. We studied a DCM (4-dicyanomethylene-2-methyl-6-p-dimethylaminostyryl-4H-pyran) dye solution in dimethyl sulfoxide (DMSO). DCM is a well-known dye which has been extensively used as laser dye, because of its high quantum yield [19]. For this application, it offers the additional advantages of a high two-photon absorption cross-section and a large Stokes-shift. This last property is important in STED microscopy to ensure that the stimulation beam does not induce one-photon absorption. In our case, even larger Stokes-shifts are required since the same wavelength is used to generate two-photon transitions, so the stimulation wavelength should be close to twice that of the linear absorption peak. In the following, we demonstrate that a two-photon excited population can be depleted by stimulated emission at the excitation wavelength. The depletion efficiency has been studied using time-resolved fluorescence intensity measurements by time-correlated single photon counting (TCSPC). We also performed numerical simulations to investigate quantitatively the

influence of experimental parameters in the excitation/depletion process and estimate the resolution enhancement that can be achieved by SW-STED.

2. Theory

A schematic representation of two-photon absorption and STED process is shown in Fig. 1. The molecule is initially excited from the low vibrational levels in the S_0 ground state by the simultaneous absorption of two photons, followed by rapid relaxation to lower vibrational levels in excited singlet state S_1 . Without external perturbations, the population in S_1 decays by spontaneous emission and fluorescence can be observed. Here a second laser pulse is sent to induce stimulated emission and dump the population in S_1 to the upper vibrational levels of S_0 before fluorescence emission can occur.

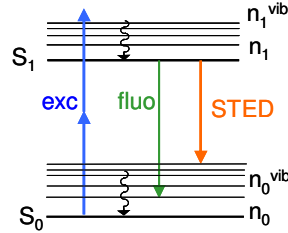


Fig. 1. Energy levels and optical transitions involved in SW-STED.

A complete theoretical model for STED including the population anisotropy created by the polarized excitation and depletion pulses would be complex and outside the range of this work. This polarization effect has been described by other authors [20,21]. We shall only keep in mind that the efficiency of STED is mainly affected by three factors: *a*) the viscosity of the solvent, which controls the speed of reorientation of excited molecules; *b*) the delay between the excitation and stimulation pulses and *c*) the angle between the polarizations of the excitation and STED beams. The best efficiency is obtained when the polarizations of exciting and depleting beams are parallel and when the delay is short and the viscosity sufficiently high to prevent molecular reorientation.

In the present description, we consider the simplified case where the anisotropy due to pulse polarization is not present. Under this approximation, we used the following set of equations to describe the population evolution in the four levels (n_0 and n_1 are the populations of the low lying vibrational levels of S_0 and S_1 respectively, whereas n_0^{vib} and n_1^{vib} refer to the upper vibrational levels of the same states):

$$\frac{dn_1^{vib}}{dt} = \sigma_{TPA}(I_{femto}^2 + I_{pico}^2)(n_0 - n_1^{vib}) - \frac{n_1^{vib}}{\tau_{vib}} \quad (1a)$$

$$\frac{dn_1}{dt} = \sigma_{STED}I_{pico}(n_0^{vib} - n_1) - n_1\left(\frac{1}{\tau_{rad}} + \frac{1}{\tau_{NR}}\right) + \frac{n_1^{vib}}{\tau_{vib}} \quad (1b)$$

$$\frac{dn_0^{vib}}{dt} = \sigma_{STED}I_{pico}(n_1 - n_0^{vib}) + n_1\left(\frac{1}{\tau_{rad}} + \frac{1}{\tau_{NR}}\right) - \frac{n_0^{vib}}{\tau_{vib}} \quad (1c)$$

$$\frac{dn_0}{dt} = -\sigma_{TPA}(I_{femto}^2 + I_{pico}^2)(n_0 - n_1^{vib}) + \frac{n_0^{vib}}{\tau_{vib}} \quad (1d)$$

In these equations, σ_{TPA} and σ_{STED} are the two photon absorption (TPA) and the stimulated emission cross section respectively; τ_{rad} and τ_{NR} are the radiative and non radiative relaxation times of the emitting singlet state; τ_{vib} is the rapid vibrational relaxation time which is assumed to be the same for the ground state and the excited state (this assumption is justified by the fact that it is much faster than the other considered processes). Finally I_{femto} and I_{pico} are the

intensity of the fs pulses and the stretched pulses respectively. These two pulses are not temporally overlapped: the stretched pulse arrives on the sample approximately 100 ps after the fs pulse. These equations are similar to the formulation in reference [22]. However, since the excitation is induced by a two photon absorption process, its probability depends on the square of the intensity.

Two issues need to be addressed if a single laser wavelength is to be used for both excitation and depletion, as proposed in SW-STED. The first question is whether the fs pulse which role is to excite the molecules may also cause stimulated emission. This event should be very improbable, because stimulated emission can only occur from the low vibrational levels of S_1 and a delay of ~ 1 ps (represented by τ_{vib}) is needed for an excited molecule to relax to these levels. Therefore the fs pulse is too short to induce stimulation. That is the reason why we wrote only I_{pico} in Eqs. (1b) and (1c).

Secondly, the stretched (picosecond) pulse, which is meant to deplete the excited state, can also excite the molecules by two-photon absorption (hence the presence of I_{pico} in Eq. (1a) and (1d)). To avoid this problem, we have to work in a regime where stimulated emission is the dominant process. This is done by increasing the duration of the pulse: the total population excited by two-photon depends on the instantaneous intensity and will decrease, while the amount of stimulated emission does not change. In section 4, we show that it is possible to obtain an efficient depletion with a picosecond beam that does not cause significant fluorescence and, using calculations, the crossover between these two processes is analyzed in more detail.

If stimulated emission is much more efficient than spontaneous emission and provided the depleting pulse is sufficiently stretched to prevent any competing two photon process, Eq. (1b) can be simplified, as shown by Klar et al. [23]:

$$\frac{dn_1}{dt} = -\sigma_{STED} I_{pico} n_1 \quad (2)$$

In this case, the population n_1 is quenched accordingly to the following exponential law:

$$n_1 \propto e^{-\sigma_{STED} I_{pico} \Delta t} \quad (3)$$

where Δt is the duration of the stretched pulse. Therefore, the fluorescence signal should decrease exponentially as a function of the power in the STED beam. This expression will be used to obtain an estimation of the stimulated emission cross-section from the decay rate.

3. Experimental setup

The experimental setup used in our depletion experiments is shown on Fig. 2. The laser pulses for two-photon excitation and for stimulated emission of the dye, both come from a widely tunable (680-1080 nm), mode-locked Ti:sapphire laser (ChameleonTM, Ultra II) delivering linearly polarized pulses with a typical duration of 140 fs and a repetition rate of 80 MHz. The main fs pulse is split in two paths by a polarizing cube and the power distribution between the two paths can be adjusted by a half-wave plate. The first beam is used to excite the dye by two-photon absorption and the second beam is used to deplete the excited state by stimulated emission. Femtosecond pulses exhibit high peak powers and are well-suited for nonlinear excitation, but since stimulated emission is a linear process, its efficiency only depends on the total energy of the pulse. Therefore, to favor stimulated emission and avoid non-linear processes, the second pulse is temporally stretched using a pair of gratings (Newport Richardson Gratings, gold, plane holographic, 1500 grooves/mm, high blaze angle). The duration of the stretched pulse was determined from the spectral bandwidth of the laser output which was measured using a fiber spectrometer. The bandwidth was found to be 2.7 nm at 680 nm and 3.5 nm at 700 nm. We deduced the duration of the stretched pulse which is 32 ps and 45 ps at 680 and 700 nm respectively.

The temporal delay between the excitation and the depletion (stretched) pulse at the sample is adjusted using a delay line on the excitation path. No other synchronization tools are

necessary because the exciting and the depleting pulse are provided by the same laser source. The two beams are recombined by a second polarizing cube and then their polarization is made circular by a quarter wave-plate, in order to produce a more efficient depletion compared to a configuration with crossed polarizations (see further discussions in the text). The two beams are attenuated and focused by a 40x objective. (Olympus LUMPlanFL/IR, N.A. = 0.80, working distance 3.3 mm) into a 1 cm-deep quartz cell containing the chosen dye. The back aperture of the objective lens was partially covered, therefore the effective N.A. was ~0.5. Fluorescence was collected perpendicularly to the excitation and depletion beam by two 10x objectives (N.A. = 0.3). On one side the fluorescence spot was imaged on a CCD camera (PixelInk Megapixel FireWire Camera). On the other side of the cell, the signal was focused on a monochromator (Jobin Yvon H20) equipped with a GaAs photocathode micro-channel plate (Hamamatsu R3809U-61) connected to a time correlated single photon counting board (TCSPC, PicoQuant, GmbH, Berlin, Germany). A 50 μm slit was placed at the monochromator entrance, which allows rejection of out-of-focus fluorescence.

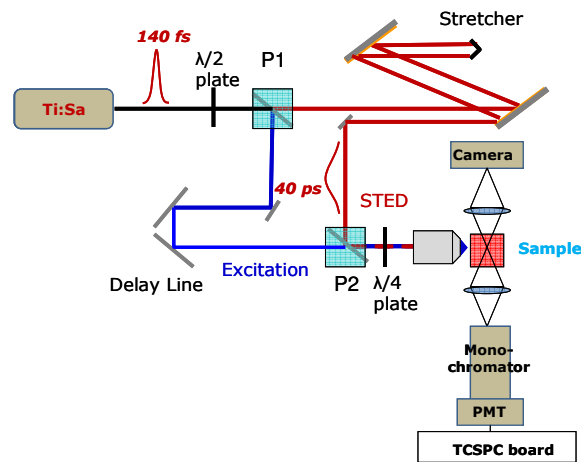


Fig. 2. The experimental setup.

Chemicals were used as received, without any further purification. DCM [2-[2-[4-(dimethylamino) phenyl] ethenyl]-6-methyl-4H-pyran-4-ylidene]-propanedinitrile was purchased from Exciton and dissolved in dimethyl sulfoxide (DMSO). DMSO was chosen for its excellent solvent properties and the fact that it has no absorption band in the range of our excitation wavelengths, preventing thus thermal lensing effect.

The TPA cross section spectrum for DCM was determined in the spectral range from 680 nm to 1000 nm by upconversion fluorescence measurements using a Ti:sapphire fs laser. The fluorescence, collected at 90° to the excitation beam, was focused into an optical fiber connected to an Ocean Optics S2000 spectrometer. The incident beam intensity was adjusted to 50 mW in order to ensure an intensity-squared dependence of the fluorescence over the whole spectral range. Calibration of the spectra was performed by comparison with the published Coumarin-307 and Rhodamine TPA spectra [24].

4. Results

The measured two-photon absorption and fluorescence emission spectra of the DCM dye are shown in Fig. 3. Our experiments are performed at 680 nm and 700 nm, near the edge of the tuning range of our laser. The two-photon cross-section was measured to be 27 GM (1 GM = $10^{-50} \text{cm}^4 \cdot \text{s}$) and 30 GM at 680 nm and 700 nm respectively.

By using the experimental set-up described above we have simultaneously recorded the fluorescence traces with the CCD camera and the fluorescence signal decays using TCSPC measurements. In the following we will refer to the fs beam as the excitation beam and to the

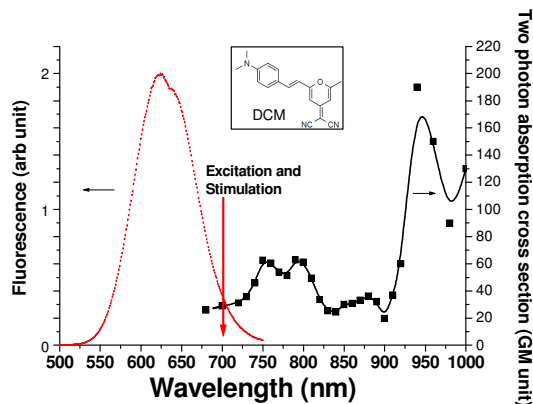


Fig. 3. DCM two-photon absorption cross section (straight line and squares) and fluorescence (dotted line) spectra in DMSO. The arrow indicates the excitation and stimulation wavelength. DCM chemical structure is shown in the inset.

ps stretched beam as the STED beam. The laser wavelength was sufficiently red shifted compared to the linear absorption spectrum of DCM to avoid important one-photon excitation. Two-photon excitation by the STED beam was prevented by stretching the pulse to 40 ps, as already mentioned. The power provided by our laser source was amply sufficient for both two-photon excitation and stimulated emission depletion.

We recorded successive images of the fluorescent focal spot of the focused excitation beam (Fig. 4a) of the focused STED beam (Fig. 4b), and finally of the two overlapped beams, focused together into the dye cell (Fig. 4c). We can clearly observe an important fluorescence quenching at the focal spot when the two beams overlap.

At the same time we recorded the fluorescence decays with our TCSPC system. In this way, we were able to adjust the delay between the two pulses in order to optimize the depletion effect. In Figs. 4d, 4e and 4f, the fluorescence signal decays corresponding to the

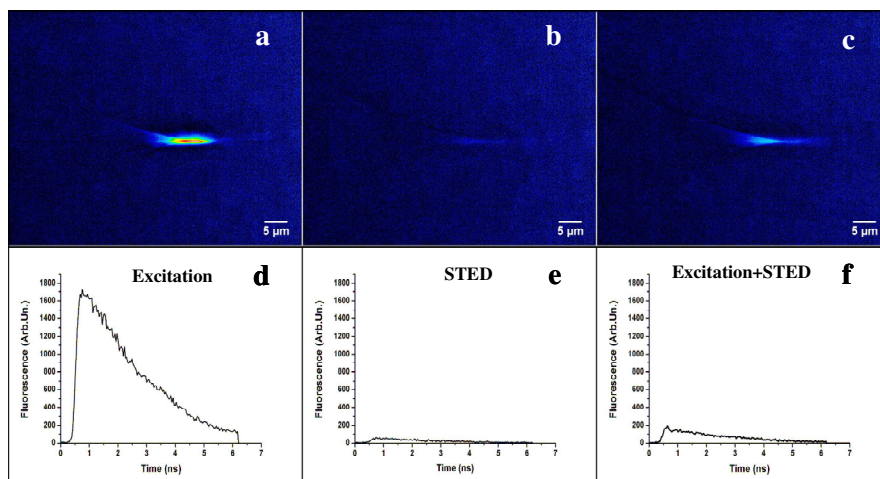


Fig. 4. Images and time evolutions of fluorescence emission in the DCM cell. Upper part: images taken with a CCD camera on the side of the sample cell inside which either the excitation beam (fs pulse) alone (a), or the STED beam (ps pulse) alone (b) are focused, or the two beams are overlapped (c). Lower part: fluorescence decays recorded with TCSPC device: (d), (e) and (f) correspond to images (a), (b) and (c) respectively. Average powers: 25 mW for excitation beam, 80 mW for STED beam.

pictures are presented. When only the excitation beam is focused in the sample, we observe a typical fluorescence decay (Fig. 4d). A fluorescence lifetime of $\tau = 2.18$ ns has been determined using a linearly polarized excitation beam. This value is in perfect agreement with previous measurements [25]. With the STED beam alone, almost no fluorescence signal can be detected (Fig. 4e). When the two beams overlap, the fluorescence signal created by the excitation beam was quenched to less than 10% (Fig. 4f).

In order to rule out the possibility of secondary effects such as thermal lensing, which would defocus the pump beam and reduce the efficiency of two photon absorption, we have intentionally delayed the STED beam by a small lapse of time (0.5 ns) as shown in Fig. 5. Clearly, it can be observed that fluorescence quenching occurs only in concordance with the STED pulse. No cumulative effect from one pulse to the following was observed. Therefore we could exclude the occurrence of undesired thermal effects. Moreover, after quenching, the fluorescence decay remains a single exponential with an unchanged time constant, only the signal amplitude is affected. This is a signature of stimulated emission depletion, and has been observed previously [21,26].

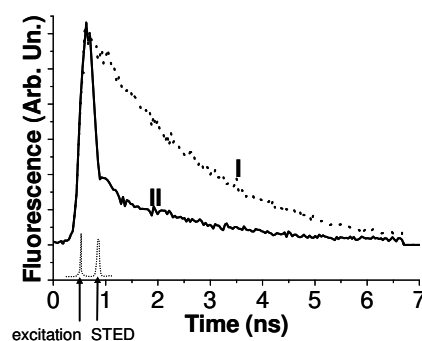


Fig. 5. Two-photon excited fluorescence quenched by a STED pulse delayed of 0.5 ns: (I) fluorescence decay without STED pulse; (II) fluorescence decay in presence of the STED pulse.

Depletion efficiency is known to depend on relative polarization between excitation and depletion beams. We compared the depletion effect obtained using two beams with crossed polarizations (Fig. 6a) and circular polarization (Fig. 6b) at the same power. As expected, the quenching is less efficient in the case of crossed polarization: after the first pulse, the excited molecules are preferentially aligned parallel to its polarization; if the STED beam has a perpendicular polarization, only the molecules that have rotated in the solvent could be depleted. Since few molecules have had time to rotate in the short delay between the two pulses, the depletion efficiency is low. This effect is in agreement with previous theoretical work. When circularly polarized beams are used, a more efficient quenching can be observed as shown on Fig. 6b, since this reorientation problem is not present. Therefore, all the results presented hereafter are obtained using circularly polarized beams.

In the theoretical section, we have shown that, as long as the STED beam does not cause significant two-photon absorption, the total fluorescence is expected to decrease exponentially with increasing STED power (Eq. (3)), as reported in previous two-wavelength STED experiments [23]. To verify this assertion and estimate the stimulated emission cross-section, we carried out experiments in which the excitation pulse power was kept constant at 25 mW and the STED pulse power was varied from 10 mW to 80 mW at 680 nm, and from 10 mW to 200 mW at 700 nm. The results are shown in Fig. 7. As predicted, fluorescence quenching increases exponentially with the STED beam intensity. The curve measured at 680 nm decreases more sharply than that measured at 700 nm, which indicates a more efficient depletion. This is in agreement with Eq. (3): since the spectral dependence of stimulated

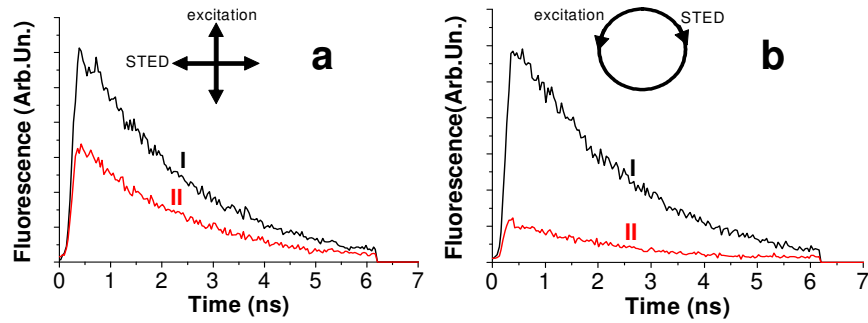


Fig. 6. Depletion efficiency for excitation and STED beams with crossed polarization (a) and circular polarization (b). In both graphs, (I) is the undepleted decay (no STED beam) and (II) is the fluorescence decay in presence of the STED beam.

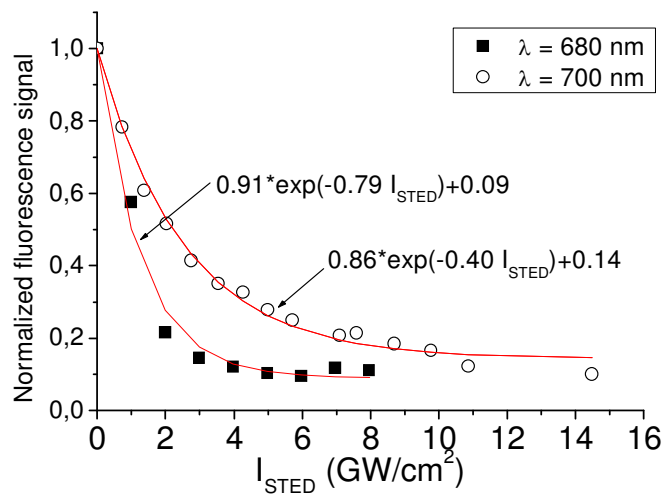


Fig. 7. Fluorescence depletion as function of the peak intensity of the focused STED beam for excitation/stimulation at 680 nm (filled squares) and 700 nm (circles).

emission cross-section σ_{STED} is similar to the fluorescence emission spectrum (shown on Fig. 3) as it has been experimentally demonstrated in previous studies [27,28], when changing the wavelength of excitation-stimulation from 680 nm to 700 nm, σ_{STED} is reduced by close to a factor of 2.

Using the exponential fit to the data and the STED pulse duration which is 32 ps and 44 ps for 680 nm and 700 nm respectively, the stimulated emission cross-section can be estimated for the two wavelengths:

$$\sigma_{STED} = 7.10^{-18} \text{ cm}^2 @ 680 \text{ nm}$$

$$\sigma_{STED} = 3.10^{-18} \text{ cm}^2 @ 700 \text{ nm}$$

These values are in good agreement with typical cross sections of allowed transitions in dye molecules and previous data for DCM molecule [29].

The data shown on Fig. 7 exhibit an offset which is not predicted by the simple model of Eq. (3). Approximately 10% of the fluorescence signal could not be depleted. This offset could be partly attributed to experimental parameters such as imperfect overlapping between

the two focused beams. However, as we will show in the following paragraphs, the fraction of population that can be depleted is intrinsically limited in the SW-STED method.

In order to better understand the depletion mechanism, we have performed numerical calculations using the coupled rate equations presented in the theoretical section. Assuming that all the molecules are initially in the lower ground state vibrational levels, the populations of the four levels were evolved step by step (time interval of 20 fs) according to the rate equations. The fluorescence signal is supposed to be proportional to the time-averaged population (n_l) of the excited state low vibrational levels. In the calculations, photophysical constants have values close to our experimental conditions at 680 nm. The two-photon absorption cross-section σ_{TPA} was 27 GM as determined experimentally. The radiative τ_{rad} and non-radiative τ_{NR} relaxation time were deduced from the fluorescence lifetime we have measured ($\tau = 2.18$ ns), assuming a quantum yield of 0.8 [25]: we obtain $\tau_{\text{rad}} = 2.7$ ns and $\tau_{\text{NR}} = 11$ ns. We used the stimulated emission cross-section value estimated above. The fast vibrational relaxation was supposed to be ~ 1 ps, in agreement with previous work on molecular dyes [21,30]. Laser pulse durations and delay are the same as in our experiments.

First we calculated the fluorescence depletion as a function of the STED instantaneous intensity. The result for the wavelength of 680 nm is shown in Fig. 8. For low STED intensity, the fluorescence signal decreases exponentially, in agreement with our experimental measurements. This behavior is similar to the one observed previously for two-wavelength depletion measurements [23]. However, as the STED intensity is increased, the intensity signal no longer follows this exponential decay but increases again. This is due to two-photon transitions induced by the STED beam. Two-photon excitation probability varies as the square of the intensity, whereas stimulated emission increases linearly. Therefore, if the STED intensity is increased beyond a certain level, two-photon absorption will become dominant and generate significant fluorescence signal. The cross-over intensity level depends on the ratio between the cross-sections of two-photon absorption versus stimulated emission. The minimum residual fluorescence signal should be 3% in our experimental conditions. This value can be reduced by further stretching the STED pulse duration. When comparing with the experimental curve at 680 nm in Fig. 7, we can see a good agreement in the order of magnitude of I_{STED} : the experimental data being limited to the region below 8 GW/cm² (limited by our laser power), the rise of fluorescence was not observed, in agreement with the calculated curve. Moreover, part of the offset in the experimental curve (9% of the initial fluorescence signal) can be accounted for by the onset of two-photon excitation induced by the STED beam which leads to a residual fluorescence of 3% as shown in Fig. 7. The remaining 6% should be attributed to other factors such as non-perfect overlapping of the two beams or orientational relaxation of the molecules in the time lapse between the two pulses, which may reduce the depletion efficiency [31].

Although the single-wavelength approach we propose does not allow total fluorescence extinction, it is possible to obtain substantial resolution enhancement as discussed in the following. To calculate the point spread function (PSF) of a microscope based on the SW-STED principle, we assume the excitation beam has a Gaussian profile of the form $\exp(-2x^2/\omega^2)$ where $\omega = \lambda/(2NA)$ and the STED beam exhibits zero intensity in the center. For simplification, the STED profile was supposed to be that of a standing wave: $\sin^2(\pi x NA/\lambda)$. Here, we suppose that a pinhole is present in the image plane in front of the detector like in a confocal microscope, although many two-photon microscopes use large area detectors. This pinhole is useful to reject unwanted fluorescence from either one-photon or two-photon absorption of the STED beam. In this case, the overall PSF is given by the product of the excitation PSF by the detection PSF. For a confocal microscope these two functions are similar in width. When fluorescence depletion occurs, the excitation PSF is changed but not the detection PSF. To take into account the depletion effect, the fluorescence profile was calculated for each abscissa x by solving the rate equation numerically using the same parameters as in Fig. 8. Then, it was multiplied by the detection PSF which is supposed

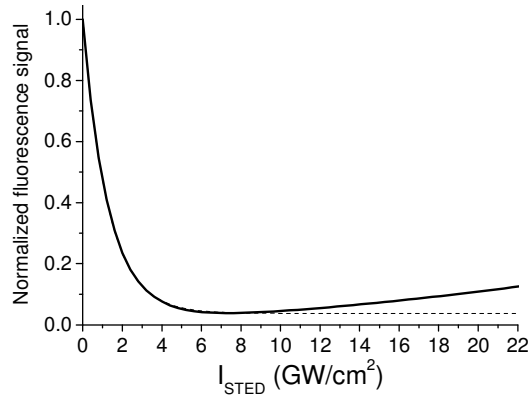


Fig. 8. Calculated fluorescence depletion as a function of STED beam intensity in the single wavelength scheme (solid line). The beginning of the curve was fitted by an exponential decay (dashed line).

to be a Gaussian similar to the excitation profile. This was done for different values of the maximum intensity in the STED profile I_{STED} , and the resultant normalized PSF is shown on Fig. 9. As the STED intensity is increased, we observe a sharp narrowing of the central peak of the PSF, which indicates a better resolution. However, for high values of I_{STED} , side lobes can be seen to grow on each side of the central peak, due to two-photon absorption of the STED beam. This is the same phenomenon as the rise of fluorescence in the curve on Fig. 8. Although the presence of side lobes will cause each bright spot to be surrounded by a ring in the images, we believe it does not fundamentally limit the resolution enhancement, since a better image could be recovered by deconvolution. A reliable way to assess the intrinsic resolution of an optical system is to use the optical transfer function (OTF) which describes the strength with which each spatial frequency of the object is transferred to the image. The resolution is given by the highest spatial frequency that can be passed above noise level. We obtained the OTF by calculating the Fourier transform of the PSF. They are shown on Fig. 9 for different values of I_{STED} (the same normalization factor is used for all four curves). When the STED intensity increases, the amplitude of the OTF decreases since the fluorescence signal is quenched, but the bandwidth is significantly enlarged which clearly indicates an improvement of the resolution of the microscope. Therefore, in the SW-STED approach,

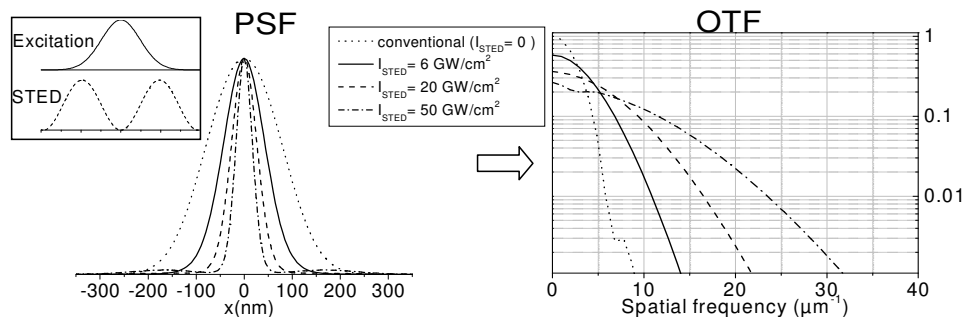


Fig. 9. Calculated point spread function (PSF) and optical transfer function (OTF) for a SW-STED microscope with increasing peak intensity in the STED beam (the case $I_{\text{STED}} = 0$ corresponds to a conventional two-photon microscope with a pinhole). The excitation and STED beam profiles are shown in the inset. The calculations are based on a NA = 1.4 microscope objective, a laser wavelength of 680nm and a configuration with a pinhole in the image plane.

although reabsorption of the STED beam will have an impact on the shape of the PSF for high depletion power, it does not impair the capacity of this technique to fundamentally improve the resolution.

5. Discussion and conclusion

In this work we have introduced an alternative scheme for STED microscopy that we have named SW-STED (Single Wavelength STimulated Emission Depletion). In our approach, two photon excitation and stimulated emission are induced using a unique wavelength from a single laser source (a Ti:sapphire laser oscillator). We have demonstrated the possibility to quench two-photon excited fluorescence by stimulated emission with a single wavelength. Time-resolved fluorescence intensity measurements were used to ascertain that the observed quenching is due to stimulated emission and not thermal or other photochemical effects since fluorescence extinction and recovery are in the ps range, in addition the effect is perfectly reversible. The amount of quenching as a function of the STED intensity follows an exponential law, as predicted and seen in previous literature [23]. In our experiment, the intensity necessary for depletion was relatively high (approximately 1 GW/cm² for 50% fluorescence depletion). This could certainly be improved by further stretching the duration of the STED beam: it was only 32 ps long in our experiment. Since stimulated emission only depends on the pulse energy, if the STED pulse is stretched to 200 ps, the same depletion efficiency would be obtained with an intensity level divided by 6 (meaning 160 MW/cm² for 50% fluorescence depletion). Another option would be to better match the fluorophore emission spectrum and the laser wavelength.

In SW-STED, the wavelength used for depletion is the same as the one inducing two-photon excitation. Therefore, we have to face the potential problem of fluorescence excitation by the STED beam. Since two-photon absorption increases as the square of the STED intensity whereas stimulated emission probability varies linearly, the first process will become dominant for high intensity levels. We have examined this problem using numerical simulations and found that it is not a fundamental obstacle to resolution improvement. A good microscope configuration would include a pinhole in the image plane in order to reject fluorescence signal outside the focused spot. This pinhole would also reject any one photon excited fluorescence generated by the STED beam.

Even for high depletion powers, we have observed a small fraction of residual fluorescence that is not explained by the theory. This can probably be attributed to the imperfect overlap between excitation and STED beams. For example, the distortions of the STED beam wavefront introduced by the gratings may affect the profile of the STED beam at the focal point. This could be easily corrected by using a spatial filter to clean the wavefront. However, we believe this residual fluorescence will not affect the imaging capabilities of SW-STED microscopy since highly resolved cell imaging has already been performed with a higher fluorescence offset [16].

Although for the present study we have used DCM dye, this fluorophore is not the only good candidate. The SW-STED method can be extended to other fluorophores, the main requirements being a large Stokes-shift and sufficient overlap between fluorescence emission and two-photon absorption spectra. For example, Pyridines [32] and Styryl [33] dye families exhibit large Stokes-shifts and two-photon absorption cross-sections and have already been used successfully in STED microscopy. For live cell imaging, interesting options include large Stokes-shift red fluorescent proteins [34].

In conclusion, we have presented an experimental proof of SW-STED in solution. We believe that this concept could be applied to super-resolved microscopy by making it possible to turn a standard TPE microscope into STED microscope at low cost, since the Ti:sapphire laser that is commonly used as an excitation source in TPE microscope could also supply the STED beam. One would only need to add a device to stretch the STED pulse and adjust the delay between the two pulses. By employing one wavelength from a single laser, the problems caused by chromatic aberrations of the optics and accurate synchronization of different sources can be avoided. Moreover, since the incident wavelength can only generate two-

photon absorption, photo-bleaching and photo-toxicity should be restricted to the focal spot, even at higher powers.

Acknowledgments

T.S. acknowledges a doctoral fellowship from the Nanosciences Foundation, Grenoble, France.